Journal of Scientific Exploration, Vol. 21, No. 1, pp. 47–66, 2007 0892-3310107

Time-Series Power Spectrum Analysis of Performance in Free Response Anomalous Cognition Experiments

PETER A. STURROCK[a] AND S. JAMES P. SPOTTISWOODE[b]

[a]Center for Space Science and Astrophysics
Stanford University, MC 4060
Stanford, CA 94305
e-mail: sturrock@stanford.edu

[b]Nielsen Entertainment
6255 Sunset Blvd.
Los Angeles, CA 90028
e-mail: james@jsasoc.com

Abstract—We analyze a database of 3,325 free response anomalous cognition experiments, using procedures recently used in an analysis of a catalog of UFO events. A histogram analysis shows evidence of a significant annual modulation in the success rate, but no significant evidence for modulations associated with time of day or local sidereal time (LST). The salient feature of a power spectrum formed by the Lomb-Scargle procedure is a peak at a frequency very close to twice the lunar synodic frequency. The probability that this feature occurs by chance is estimated to be 0.03%. A running-wave analysis indicates that this is an astronomical effect rather than a spurious property of the database. We also find a peak in the power spectrum with a period of one year. This could be associated with an LST effect, but the running-wave test, which is designed to distinguish between a real LST effect and a spurious LST effect, does not support this interpretation.

Keywords: consciousness—parapsychology—anomalous cognition—physical correlates—moon

1. Introduction

Spottiswoode (1997) analyzed a database of 1,468 free response trials of anomalous cognition experiments, examining the effect size as a function of local sidereal time. He found that the effect size increased by 340% for trials within 1 h of 13.5 h LST ($p = 0.001$) compared with the mean effect size. He also analyzed an independent database of 1,015 similar trials that showed an increase in effect size of 450% ($p = 0.05$) within 1 h of 13.5 h LST. Spottiswoode considered possible artifacts due to the non-uniform distribution of trials in local time and variations of effect size with experiment but found that these appeared not to account for the effect.

We here analyze a database of 3,325 trials, which includes the earlier data and adds some experiments which were not previously available, using a procedure

recently used in an analysis of a catalog of UFO events (Sturrock, 2004). The methods used to calculate effect sizes can be found in Spottiswoode (1997). The key purpose of this procedure is to distinguish between a genuine LST effect and an apparent (but spurious) LST effect caused by an interplay of a non-uniform effect size as a function of hour of day (HOD) and a non-uniform effect size as a function of "hour of year" (HOY), where a calendar year is divided into 24 equal periods referred to, for convenience, as "hours." We examine this distinction by carrying out a "running-wave" power spectrum analysis that can potentially distinguish a genuine LST effect from a spurious LST effect.

We present some basic properties of the database in Section 2, and we carry out a periodogram analysis, using the Lomb-Scargle procedure, in Section 3. We find that the salient peak occurs at a frequency very close to twice the synodic frequency of the Moon. In Section 4, we analyze the database by means of the "running-wave" power spectrum procedure used in our UFO analysis. This analysis tends to confirm that the peak in the Lomb-Scargle power spectrum is indeed due to a lunar influence. We carry out a Monte Carlo significance test in Section 5, which indicates that the feature is significant at the level $p = 0.0003$. We discuss our results in Section 5.

For readers not familiar with power spectrum analysis, we may explain that it is a procedure for searching systematically for periodicities in a dataset. For instance, if the air pressure were to be recorded one million times a second near a piano when one strikes the middle-C key, the measurements would be found to vary with a frequency of 262 Hz (cycles per second). However, the variation is not a pure sine wave: for instance, the amplitude of the fluctuation varies with time, and one would find fluctuations also at the harmonics [2×262, 3 X 262, etc., Hz]. A "power spectrum" provides a visual display of all of the periodic modulations that are part of the "time series"—in this case, the sequence of pressure measurements. There would be a peak, of finite width, at 262 Hz (or higher or lower if the piano is off-key), and smaller peaks at 524 Hz, 786 Hz, etc. Power spectra (in cycles per year rather than cycles per second) will be found in Figure 9, etc.

2. Basic Patterns

In time-series analysis, it is prudent to examine the basic patterns in the data. We show the distribution of trials in hour of day (computed as "solar time" rather than "local time") in Figure 1. It is no surprise that the main part of the histogram extends from 8 am until 5 pm, with a lunch-time dip in the distribution from noon until 2 pm. The distribution of trials in hour of year is given in Figure 2. We see that the rate is greatest in the winter, and then declines through spring, summer and autumn.

It is convenient to make use of the following expression for local sidereal time in terms of hour of year and hour of day:

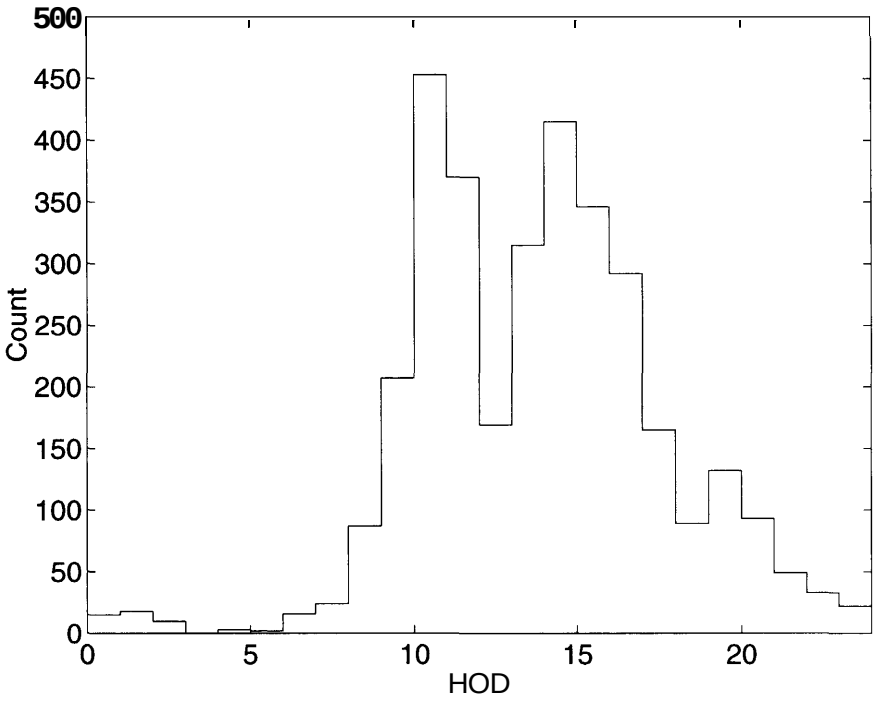

Fig. 1. Histogram formed from hour of day.

$$LST = HOD + HOY + 6.67. \tag{2.1}$$

[The factor "6.67" arises from the fact that local sidereal time is related to "right ascension." At midnight on January 1, the right ascension on the meridian is 6 h 44 m (Allen, 1973).]

The distribution of trials in LST is given in Figure 3. We see that it is V-shaped, with a minimum between 12 and 13 h.

Following our earlier article (Sturrock, 2004), we introduce the concept of "alias local sidereal time," (ALST) defined by

$$ALST = HOD - HOY + 6.67. \tag{2.2}$$

The purpose of this step is that a modulation in local sidereal time that is due to an interplay of an HOD pattern and an HOY pattern will lead also to a similar modulation in alias local sidereal time. The distribution of trials in ALST is given in Figure 4. We see that it has the form of an inverted V, with a maximum at about 15 h.

For the LST histogram and the ALST histogram, the range of the count per bin is about the same (100 to 200), so this analysis does not in itself point to an LST effect.

In Figure 5, we show the mean of the effect size Z and the standard error of the mean for the 24 hour-of-day bins. There is an appearance of a low effect size

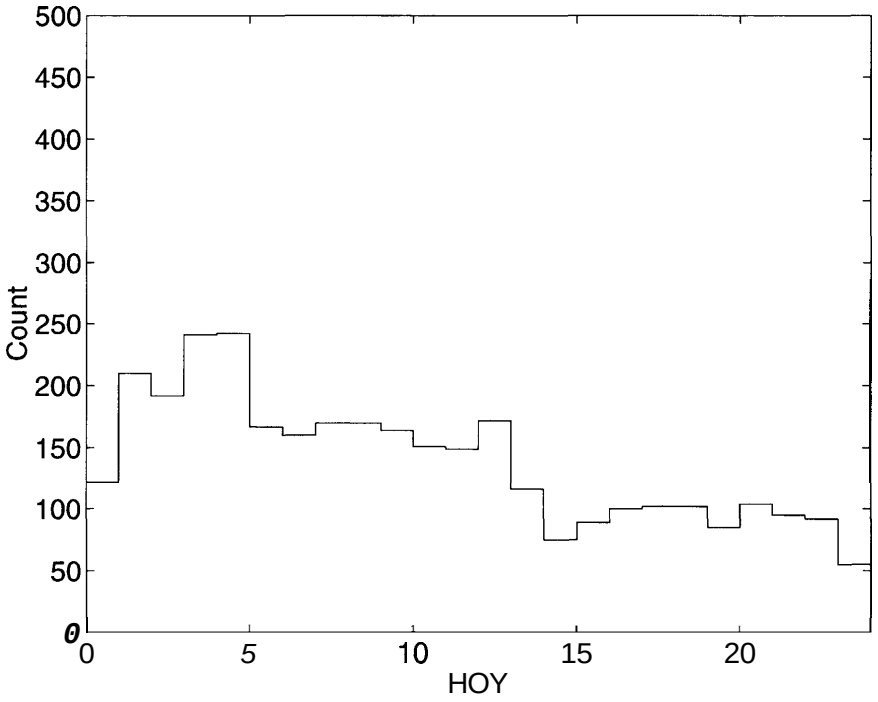

Fig. 2. Histogram formed from hour of year.

near 3–4 am and a high effect size near 7 am, but a chi-square test of all bins gives no evidence for a departure from uniformity ($p = 0.07$). In Figure 6, we show the mean of the effect size and the standard error of the mean for the 24 hour-of-year bins. There is a suggestion of a higher effect size for late May, early June, and late August, and a lower effect size for early July. A chi-square test indicates that this departure from uniformity is significant ($p = 5 \times 10^{-6}$), so this result deserves further investigation, examining different datasets separately, to determine whether this pattern appears in all experiments, or only in certain experiments. Figures 7 and 8 are similar displays for LST and ALST, respectively. Neither shows a statistically significant departure from uniformity ($p = 0.14$ and $p = 0.6$, respectively).

3. Periodogram Analysis

In any investigation of a time series, it can be helpful to examine the power spectrum. Perhaps the simplest procedure for a large but regular time series is to form the "Schuster periodogram" or "Rayleigh power" (Bretthorst, 1988; Mardia, 1972). An improved version of this operation is the Lomb-Scargle

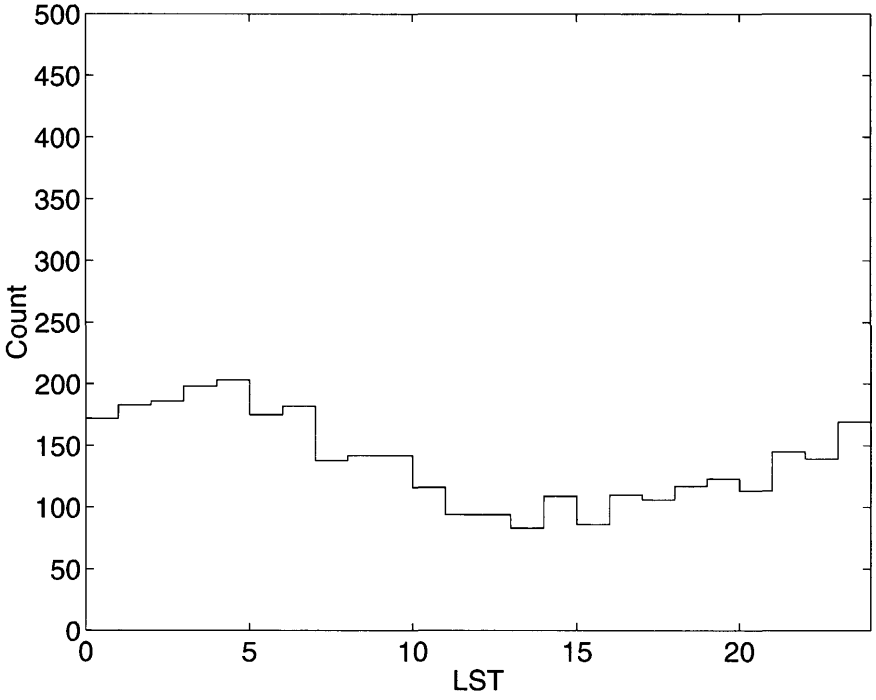

Fig. 3. Histogram formed from local sidereal time.

procedure (Lomb, 1972; Scargle, 1982), which is designed for application to time series with irregular sampling.

If we normalize the effect size values, Z_n, to have mean value zero,

$$x_n = Z_n - \text{mean}(Z_n), \tag{3.1}$$

the Lomb-Scargle power spectrum $S(\nu)$ is given by

$$S(\nu) = \frac{1}{2\sigma_0{}^2}\left\{\frac{\left[\sum_n x_n \cos(2\pi\nu(t_n - z))\right]^2}{\left[\sum_n \cos^2(2\pi\nu(t_n - \tau))\right]} + \frac{\left[\sum_n x_n \sin(2\pi\nu(t_n - \tau))\right]^2}{\left[\sum_n \sin^2(2\pi\nu(t_n - \tau))\right]}\right\}, \tag{3.2}$$

where

$$\sigma_0 = \text{std}(x_n) = \text{std}(Z_n), \tag{3.3}$$

and τ is defined by the relation

$$\tan(4\pi\nu\tau) = \frac{\sum_n \sin(4\pi\nu t_n)}{\sum_n \cos(4\pi\nu t_n)}. \tag{3.4}$$

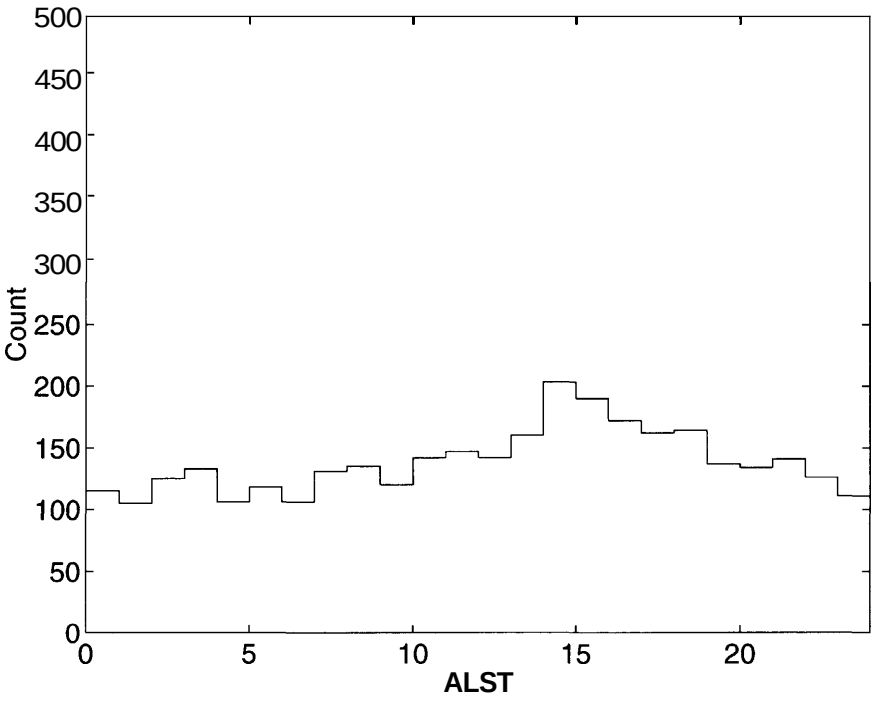

Fig. 4. Histogram formed from alias local sidereal time.

The power spectrum formed in this way from the effect size time series is shown, for frequency in the range $\nu = 0$–$5\ \mathrm{yr}^{-1}$, in Figure 9. The top ten peaks are listed in Table 1. We see that there is a peak at $1.00\ \mathrm{yr}^{-1}$ with power 5.21, but this is blended with a stronger peak at $0.95\ \mathrm{yr}^{-1}$ with power 6.02. We show in the Appendix that, as a result of the severe non-uniformity in the time series formed from trial dates, any peak in the power spectrum is likely to be contaminated by either a displacement, or the occurrence of auxiliary peaks, with separation of order $0.03\ \mathrm{yr}^{-1}$ or a small multiple of this frequency. We also find a peak at $1.98\ \mathrm{yr}^{-1}$ with power 7.29, which we may interpret as a contaminated form of a peak at $2.00\ \mathrm{yr}^{-1}$. It appears, therefore, that there is evidence for both annual and semi-annual modulations of the performance.

We have also examined the power spectrum over a much wider range $\nu = 0$–$100\ \mathrm{yr}^{-1}$. The strongest peak in this range occurs at $\nu = 24.65\ \mathrm{yr}^{-1}$, quite close to twice the synodic lunar frequency ($24.74\ \mathrm{yr}^{-1}$), with power 10.75. For clarity, we show in Figure 10 the power spectrum over the range $\nu = 0$–$30\ \mathrm{yr}^{-1}$. It is interesting to note that there is also a peak at $24.81\ \mathrm{yr}^{-1}$, since the pair of peaks at $24.65\ \mathrm{yr}^{-1}$ and at $24.81\ \mathrm{yr}^{-1}$ may be interpreted as sidebands of modulation at $24.74\ \mathrm{yr}^{-1}$ since the interval is, in each case, $0.09\ \mathrm{yr}^{-1}$, a small multiple of

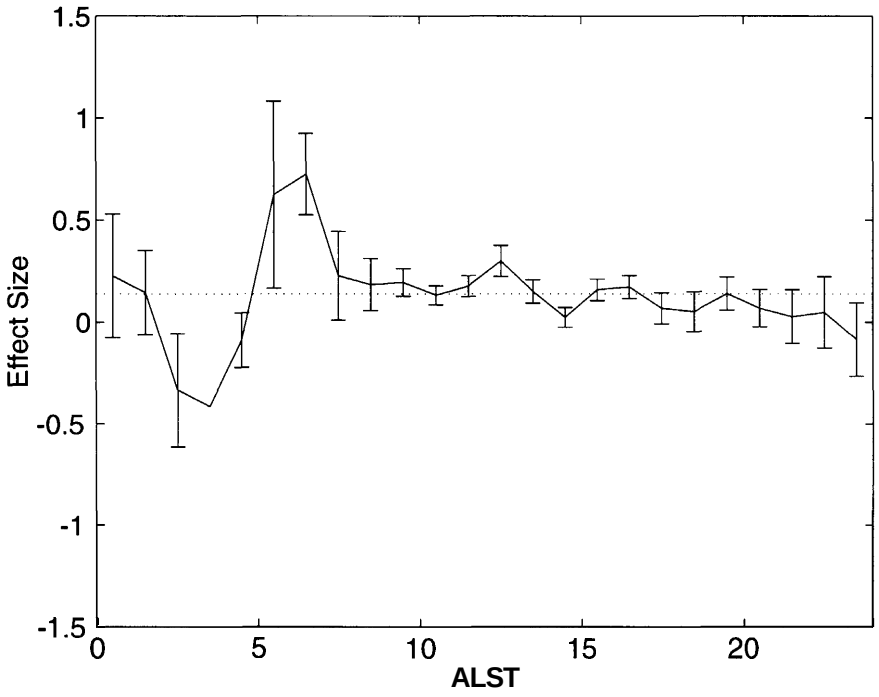

Fig. 5. Mean value of effect size and standard error of the mean for each of 24 hour-of-day bins. The dotted line denotes the mean value for the entire database.

0.03 yr^{-1}. In this connection, we may also note that there is a peak at 12.36 yr^{-1}, with power 3.34, virtually identical to the lunar frequency.

Hence Lomb-Scargle analysis of the effect size points towards modulation of the performance by a lunar-related process.

4. Running-Wave Analysis

In the previous section, we looked into the possibility that the effect size exhibits one or more oscillations in time. In this section, we ask a different but related question. We look into the possibility that the effect size exhibits a significant pattern in terms of a rotating reference frame. It is convenient to take as our basic reference frame one that is centered on the Earth, with respect to which the Sun has a fixed position. An observer on Earth would see this frame rotate with a period of one day. An observer on a nearby star would see the frame rotate with a period of one year.

With respect to this frame, we denote by φ_n the angular position of the zenith (the position looking vertically upward) at the time of trial n, but normalize the angle to run from 0 to 1:

$$\psi = \phi/2\pi. \tag{4.1}$$

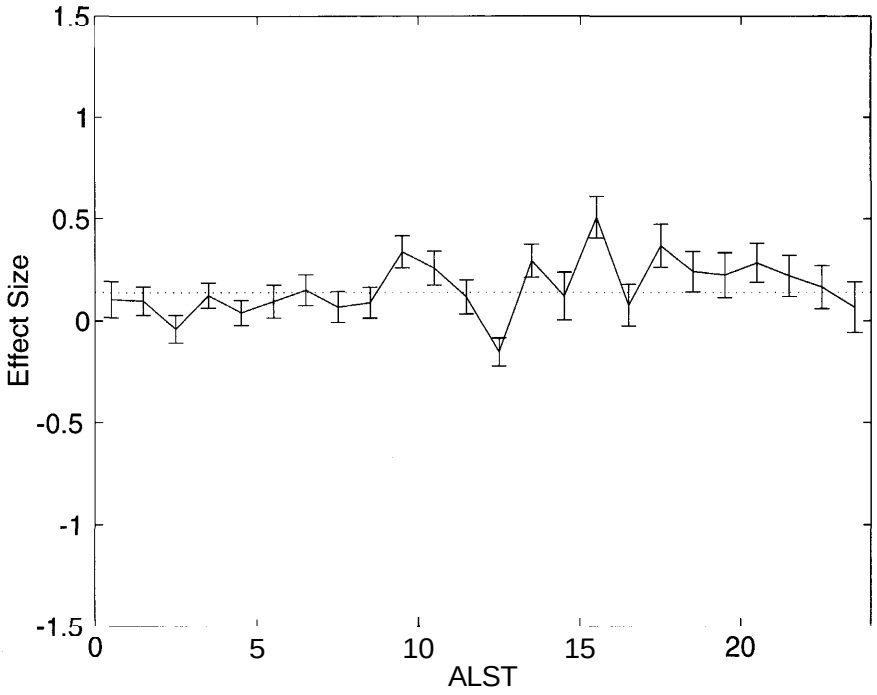

Fig. **6.** Mean value of effect size and standard error of the mean for each of 24 hour-of-year bins. The dotted line denotes the mean value for the entire database.

This quantity is related the hour of day of the trial by

$$\psi = (\mathrm{HOD})/24. \tag{4.2}$$

We now denote by v the angular velocity of the test frame with respect to the basic (Sun-locked) frame, where v is measured in cycles per year. For this analysis, it is convenient to evaluate the following form of the Rayleigh power

$$S(\mathrm{v}) = \frac{1}{N\sigma_0^2}\left|\sum_{n=1}^{N} x_n \exp[i2\pi(\psi_n + \mathrm{v}t_n)]\right|^2, \tag{4.3}$$

where t is measured in years.

We note that $\mathrm{v} = 0$ corresponds to the Sun-locked frame and $\mathrm{v} = 1\ \mathrm{yr}^{-1}$ corresponds to the star-locked frame. If t is measured from 0 h on January 1 of some year, then t is related to the "hour of year" by

$$t(\mathrm{mod}\ 1) = (\mathrm{HOY})/24. \tag{4.4}$$

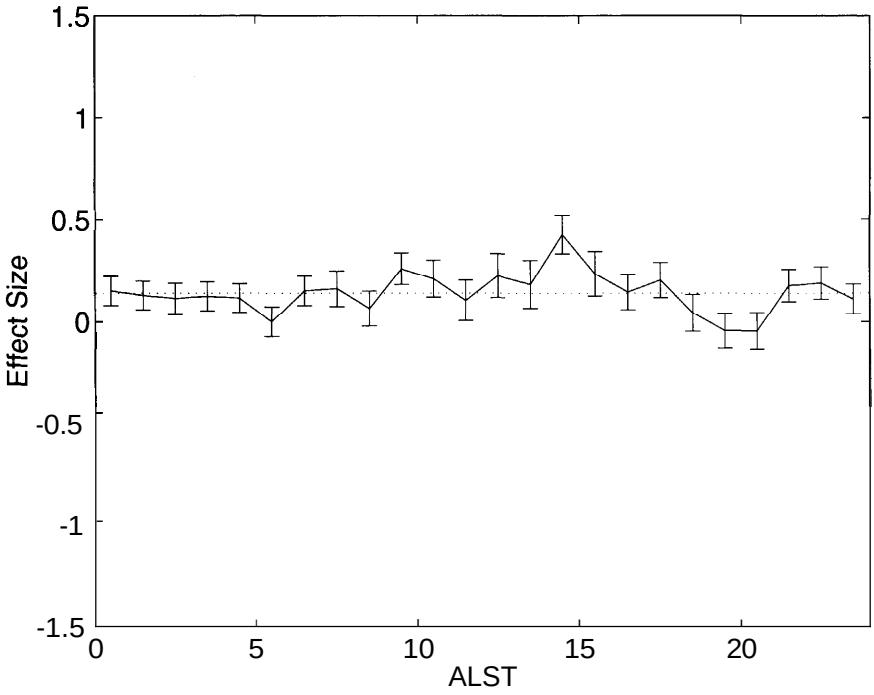

Fig. 7. Mean value of effect size and standard error of the mean for each of 24 LST bins. The dotted line denotes the mean value for the entire database.

We see from Equations 4.2 and 4.4 that, for $v = 1\ yr^{-1}$, the combination $\Psi + vt$ is effectively the sum of the hour of day and hour of year, so that it is related to the local sidereal time:

$$\psi + t(\text{mod } 1) = \frac{1}{24}(\text{LST} - 6.67). \tag{4.5}$$

Hence if there is an LST modulation in effect size values, it should show up as a peak at $v = 1\ yr^{-1}$ in the running-wave power spectrum. Similarly, if there is an ALST modulation in effect size values, it should show up as a peak at $v = -1\ yr^{-1}$ in the running-wave power spectrum. It follows that the running-wave analysis can distinguish a real LST effect from a spurious LST effect due to the interplay of an HOD modulation and an HOY modulation: the former will yield a peak at $v = 1\ yr^{-1}$ but no peak at $v = -1\ yr^{-1}$, whereas the latter will lead peaks at both $v = 1\ yr^{-1}$ and $v = -1\ yr^{-1}$ (Sturrock, 2004).

We show in Figure 11 the two power spectra for forward waves ($v > 0$) and reverse waves ($v < 0$), for the frequency range 0 to 5 yr^{-1}. The top ten peaks for the forward-wave power spectrum and for the reverse-wave power spectrum are shown in Tables 2 and 3, respectively. There appears at first sight to be a peak in the forward-wave power spectrum at $v = 1\ yr^{-1}$, with no

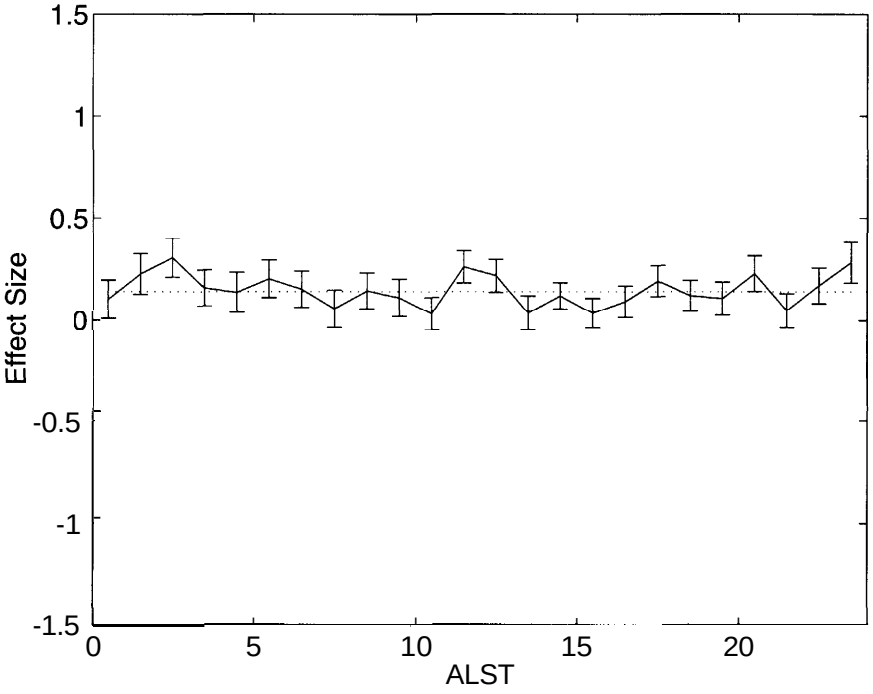

Fig. 8. Mean value of effect size and standard error of the mean for each of 24 ALST bins. The dotted line denotes the mean value for the entire database.

accompanying peak in the reverse-wave power spectrum. However, inspection of the power spectrum shows that this peak is actually at $v = 0.95\ yr^{-1}$. There is no peak at $v = 1\ yr^{-1}$ in either the forward or reverse power spectrum. Hence (in contrast to our analysis of UFO events) the running-wave analysis does not provide evidence for or against an LST effect.

In Figure 12, we show the two power spectra for forward and reverse waves for the frequency ranges $20\ yr^{-1}$ to $30\ yr^{-1}$. We find that the expected peak at $24.65\ yr^{-1}$ shows up in the reverse-wave power spectrum (with power $S = 9.77$), but not in the forward-wave power spectrum (for which the power is only 2.44). This is exactly what one would expect of a real lunar effect since, with respect to a Sun-locked frame, the Moon moves in a direction opposite to that of the stars.

5. Monte Carlo Significance Test

In order to obtain a robust significance estimate for the feature at twice the lunar synodic orbital frequency, we generate Monte Carlo simulations by means of the shuffle process. In this procedure, we shuffle either the time values or the effect size values so as to randomly re-assign effect size values among times. We will search to see how often we can find a power as large as the actual power

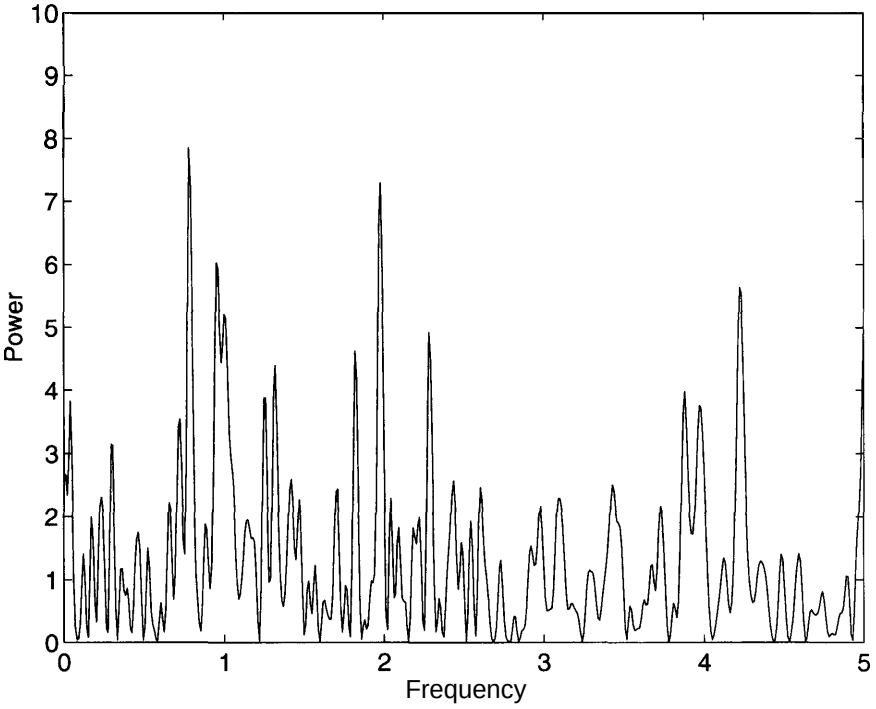

Fig. 9. Lomb-Scargle power spectrum formed from effect size values for the frequency range 0–5 yr^{-1}.

(10.75) as close to the target frequency (twice the lunar synodic frequency, 24.74 yr^{-1}) as the actual peak at 24.65 yr^{-1}. We therefore search the band 24.65–24.83 yr^{-1}. For each simulation, we compute the power spectrum over the search band, and note the power of the highest peak in that frequency range, which we denote by SM for "spectral maximum." We then examine the distribution of the maximum-power values. Figure 13 shows the distribution of values of SM from the simulations, and indicates the value of the peak in the actual data, with power $S = 10.75$. We find that only 14 simulations out of 100,000 have values of SM equal to or larger than 10.75. Hence the probability of finding a peak by chance as large as the actual peak, and as close to the target frequency as the actual peak, is 0.014%.

However, one should probably estimate the likelihood of finding a peak as large as the actual peak as close as the actual peak to either the fundamental or the harmonic of the synodic lunar orbital frequency. This increases the above estimate by a factor of two to 0.03%.

6. Discussion

The original purpose of this investigation was to review the earlier finding by Spottiswoode (1997) of an LST effect in the performance of free response

TABLE 1
Top Ten Peaks in the Power Spectrum over the Frequency Range 0 to 5 yr^{-1}

Frequency (yr^{-1})	Power
0.78	7.86
1.98	7.29
0.95	6.02
4.22	5.63
1.00	5.21
2.28	4.92
1.82	4.62
1.32	4.39
3.88	3.98
1.25	3.88

anomalous cognition experiments. Spottiswoode showed that when effect sizes were averaged in 2-h LST windows, there appeared to be a significant peak at 13.5 h LST. Spottiswoode evaluated the significance of this peak by carrying out Monte Carlo simulations, in which the effect size values were randomly permuted with respect to the LST values. In only 14 out of 10,000 simulations

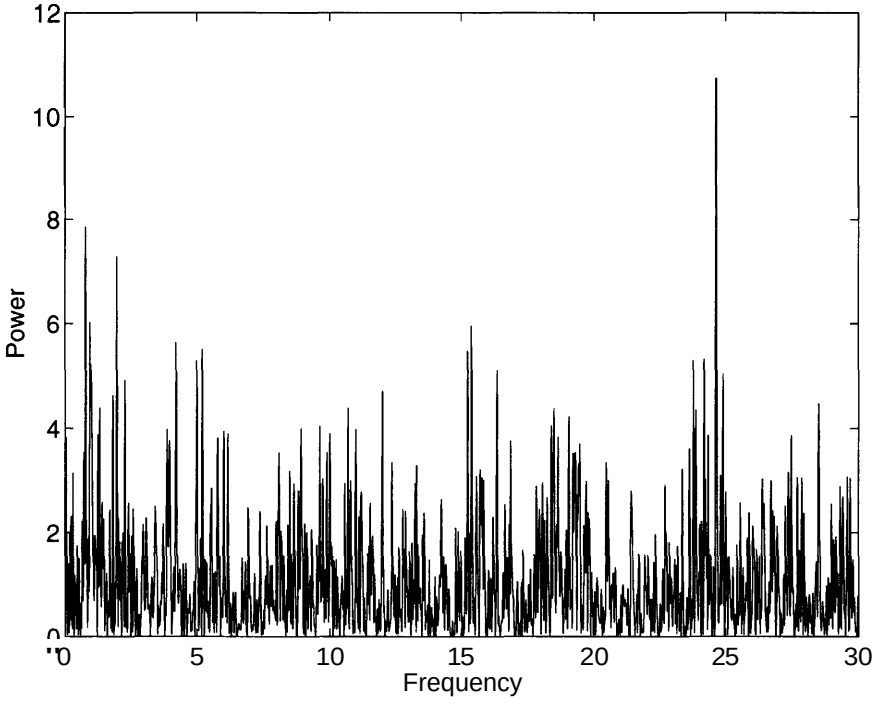

Fig. 10. Lomb-Scargle power spectrum formed from effect size values for the frequency range 0–30 yr^{-1}.

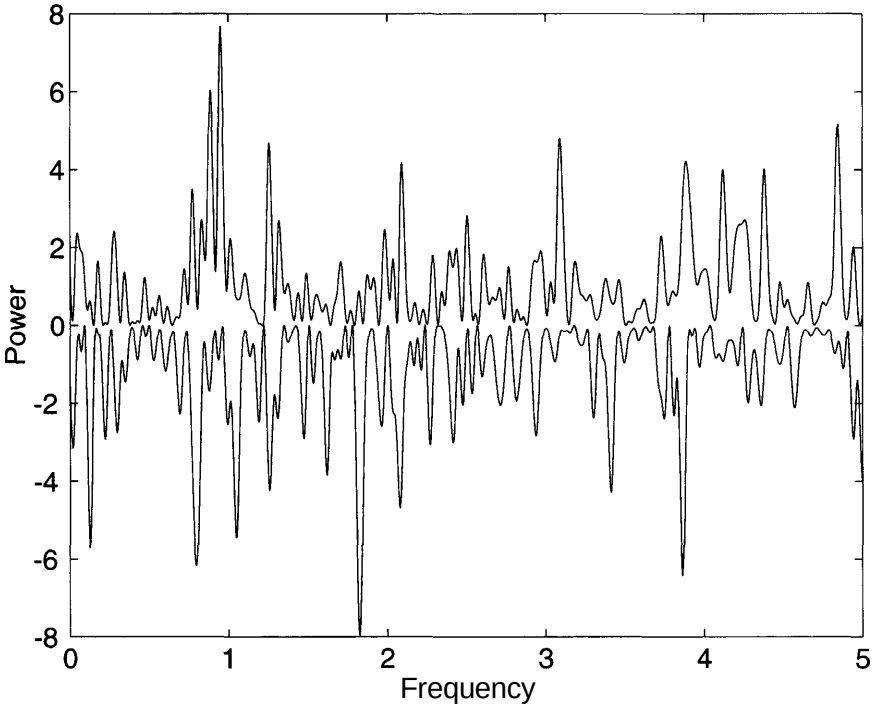

Fig. 11. Running-wave power spectrum formed from effect size values for the frequency range 0–5 yr^{-1}.

did Spottiswoode find a mean effect size as large as or larger than that of the actual dataset, implying that the feature is significant at the level $p = 0.001$. Spottiswoode's analysis has been repeated for the present expanded dataset, and the result is shown in Figure 14. The feature at 13.5 h LST appears still to be evident, but the same Monte Carlo test now gives a reduced significance level of

TABLE 2
Top Ten Peaks in the Forward Running-Wave Power Spectrum over the Frequency Range 0 to 5 yr^{-1}

Frequency (yr^{-1})	Power
0.95	7.63
0.89	6.01
4.85	5.09
3.09	4.78
1.25	4.54
3.89	4.18
2.09	4.08
4.12	3.97
4.38	3.90
0.78	3.36

TABLE 3
Top Ten Peaks in the Reverse Running-Wave Power Spectrum over the Frequency Range 0 to 5 yr^{-1}

Frequency (yr^{-1})	Power
1.82	7.93
3.86	6.34
0.80	6.17
0.13	5.65
1.05	5.30
2.08	4.69
3.41	4.28
1.25	4.16
5.00	4.06
1.61	3.72

$p = 0.01$. On the other hand, our Figure 7, derived from fixed bins rather than sliding bins, shows little evidence of an LST modulation.

Our Lomb-Scargle power spectrum analysis, shown in Figure 9, shows evidence of an annual modulation, but the results of our running-wave analysis, shown in Figure 11, are ambivalent. The forward-wave power spectrum has a peak at 0.95 yr^{-1} with power 7.63, and the reverse-wave power spectrum has

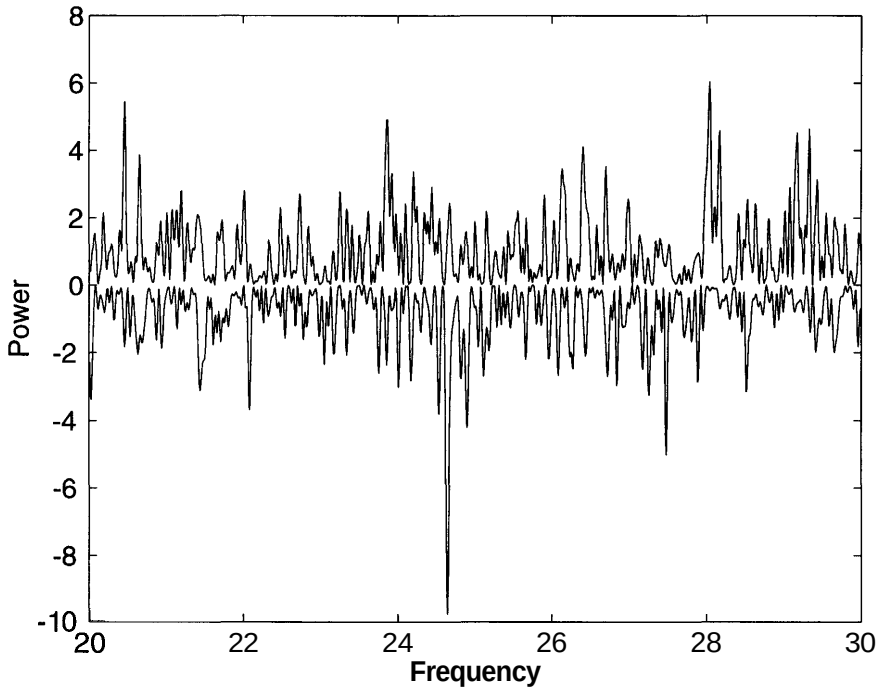

Fig. 12. Running-wave power spectrum formed from effect size values for the frequency range 20–30 yr^{-1}.

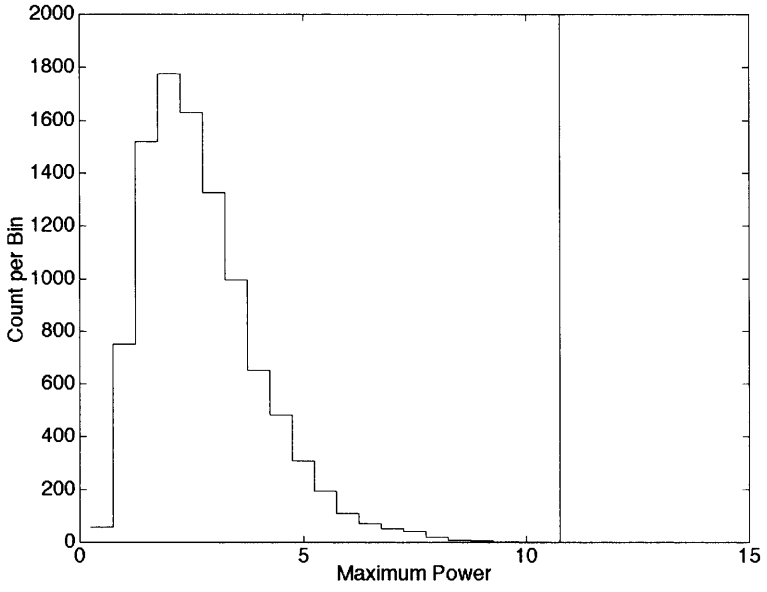

Fig. 13. Histogram formed from 10,000 Monte Carlo simulations, showing the count as a function of maximum power in the frequency band 24.65–24.83 yr^{-1}. The vertical line shows the power of the actual peak at 24.65 yr^{-1}, with $S = 10.75$. On running 100,000 simulations, we find that only 14 have $S \geq 10.75$.

a peak at 1.05 yr^{-1} with power 5.30. In order to try to evaluate the significance of this departure from the expected frequency of 1 yr^{-1}, we have carried out the analyses shown in Appendices **A** and B.

In Appendix A, we study the time-distribution of trials, and find that it is highly non-uniform. Hence we should not expect power spectra of such non-uniform time series to behave in the same way as power spectra formed from uniform time series.

In Appendix B, we study power spectra formed from Monte Carlo simulations of the time series of trial results. We find that the distribution of peak frequencies has a half-height half-width comparable with the Nyquist frequency $1/(2 \times T)$, where T is the duration of the time series. This would not explain the discrepancy between the peak frequency and the expected frequency if all trials have the same modulation. However, we find that early trials make a bigger contribution to the peak power than the later trials, so that the appropriate value of T may prove to be shorter than the value of 15–20 yr that we would infer from Figure 15. This point deserves further study, which we hope to present in a later article.

However, if we consider that the peaks at 0.95 yr^{-1} and at 1.05 yr^{-1} are relevant to our search for an LST effect, we would need to conclude that these

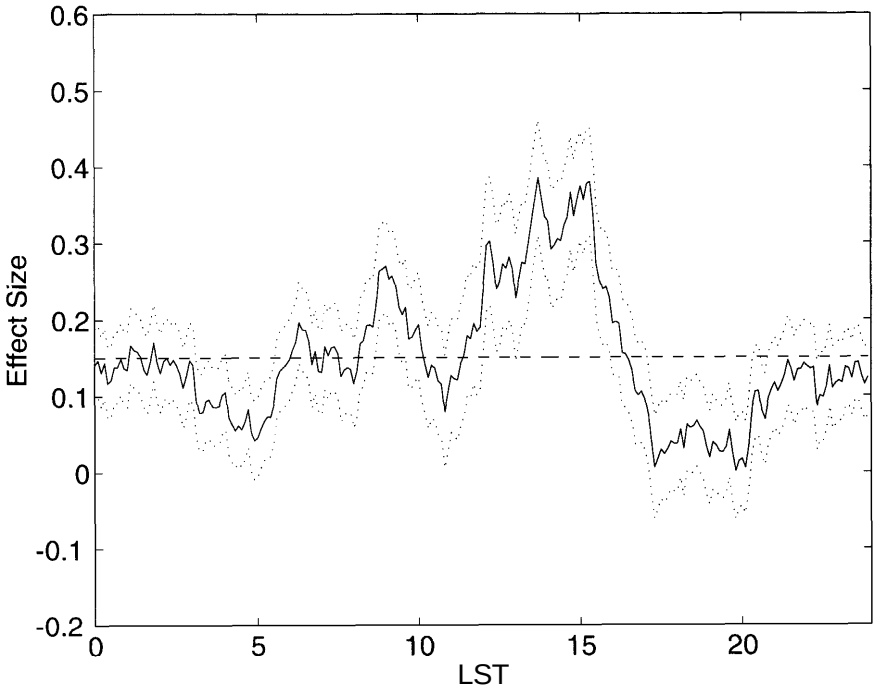

Fig. 14. Mean effect size versus LST, computed in running 2-h bins. The dotted lines indicate the departure determined by the standard error of the mean. The dashed line indicates the mean value.

results argue against a real LST effect since we find comparable powers in both the forward-wave power spectrum and the reverse-wave power spectrum.

These results leave us with the puzzle of understanding the origin of the annual modulation shown in Figures 6 and 9. It will probably be accepted that the psychological state of a person varies with the seasons. The main effect seems to be a fall-off in performance from late May to early July. It would be interesting to try to determine whether performance in anomalous cognition experiments depends on psychological state.

The surprise in this study was clear evidence for a lunar modulation of performance in anomalous cognition experiments, although we note that evidence for a lunar modulation of psi phenomena has been reported previously by Radin and Rebman (1994). The Monte Carlo test of Section 5 indicates that this feature of the power spectrum could occur by chance with a probability 0.03%. Furthermore, the running-wave analysis of Section 4 shows a clear asymmetry in the strengths of the forward and reverse waves, in the same sense that we expect of a real lunar modulation.

We are faced with the puzzle of trying to understand the small discrepancy between the frequency of the principal peak in the power spectrum (at 24.65 yr^{-1})

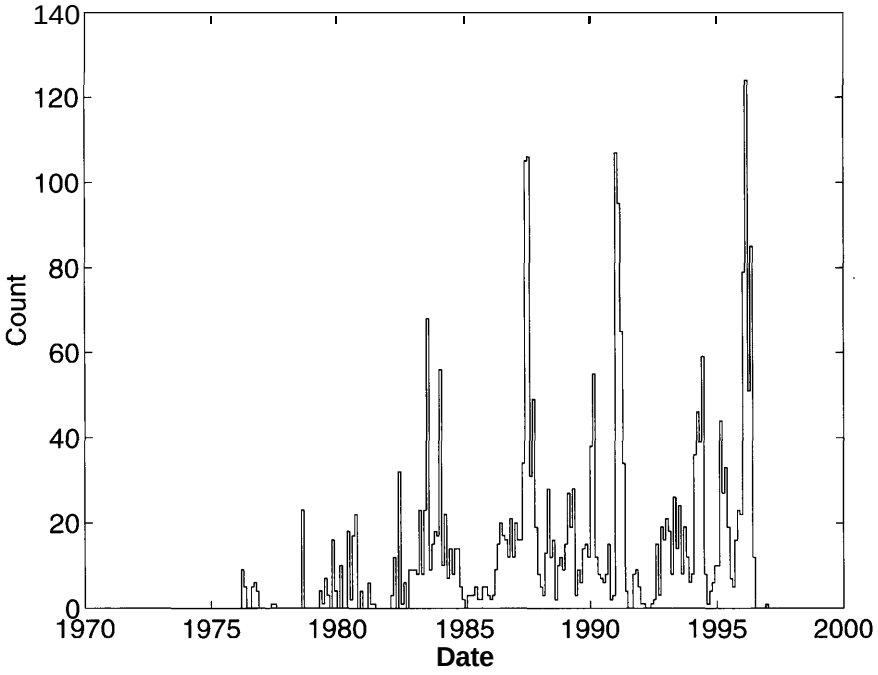

Fig. 15. Count of number of trials in bins of width 0.1 yr.

and twice the lunar synodic frequency (at 24.74 yr^{-1}). (The lunar synodic frequency is the orbital frequency of the moon as seen from Earth, which is the same as the frequency of the phase of the moon.) We find that the amplitude of this modulation is not constant, being stronger for earlier times and weaker for later times. Such a time variation can lead to sidebands, and it is possible that what we have detected is such a sideband.

Apart from this discrepancy, the mechanism of a lunar modulation is a puzzle and, to the best of our knowledge, there is no known mechanism that could explain this effect. We have looked briefly into the possibility that the effect might be attributed to fluctuations in the geomagnetic field. However, a search for lunar modulation of the geomagnetic field at the time of a lunar eclipse by Fraser-Smith (1982) yielded evidence of only very slight fluctuations. We have carried out a Lomb-Scargle power spectrum analysis of the ap and Ap indices for the time interval of the anomalous cognition database, and found no evidence of modulation at the lunar synodic frequency or its harmonic. It therefore seems unlikely that the lunar modulation can be attributed to fluctuations in the geomagnetic field.

There have, of course, been many suggestions that the phase of the moon can have psychological consequences. If this is true, and if the variation in the success rate of trials can be attributed in part to psychological processes, this combination could possibly explain the modulation that we have found.

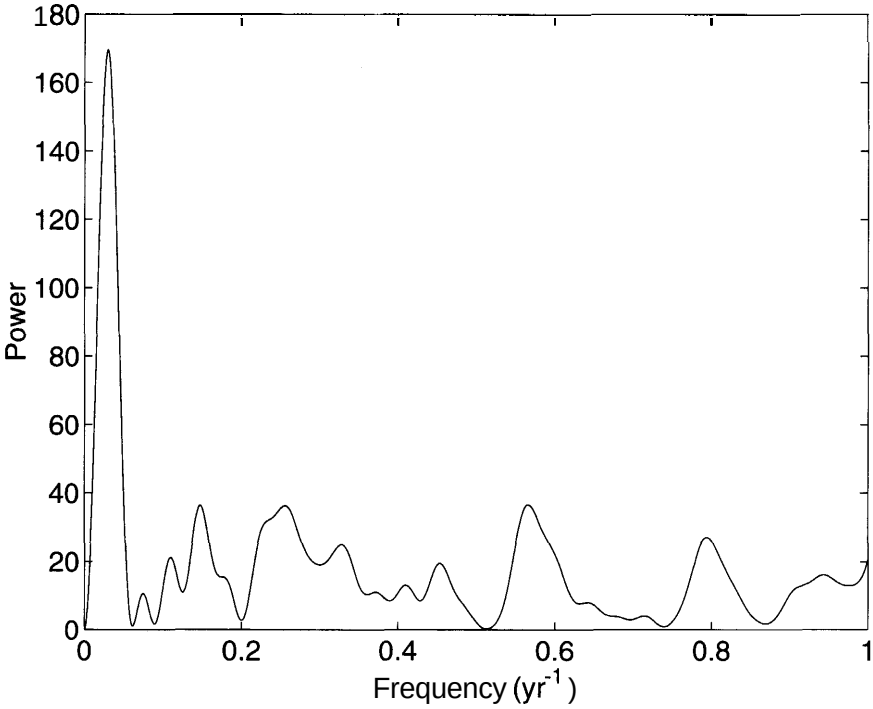

Fig. 16. Power spectrum formed from the count of number of trials in bins of width 0.1 yr.

Acknowledgments

We thank the experimental teams who have generously shared their data with us.

Appendix A

In order to help interpret the power spectra, it is helpful to examine the time series of trials. If the time series is uniform, the interpretation of the power spectra is straightforward. However, if the time series is non-uniform, the power spectra may be contaminated by aliases or sidebands.

Figure 15 shows the number of trials in bins of width 0.1 yr. We see that the time series is far from uniform. There are four prominent peaks, with separation of approximately 4 yr, which leads us to suspect that a power spectrum analysis of this time series may show a structure with a frequency scale of the order 0.25 yr^{-1}.

Figure 16 shows the power spectrum of this time series, computed by the Rayleigh power procedure (Bretthorst, 1988; Mardia, 1972). We see that there are many strong peaks within the band 0–1 yr^{-1}, with power 30 or more, including one peak at 0.25 yr^{-1} as expected, and there is one very strong peak (with power 170) at 0.03 yr^{-1}.

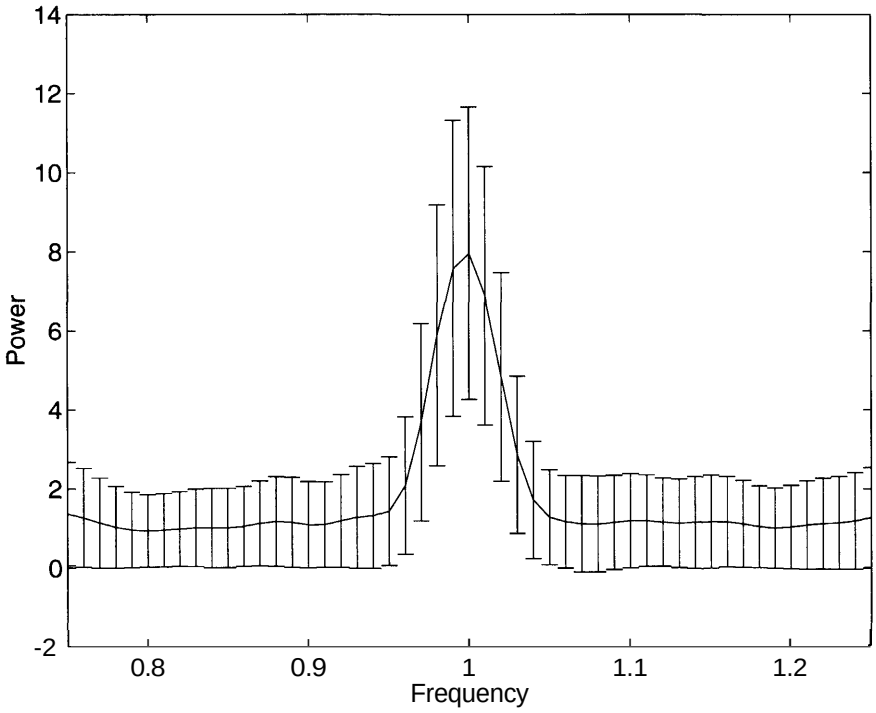

Fig. 17. Error-bar display of power spectra formed from 1,000 Monte Carlo simulations of time series with 10% depth of modulation at frequency 1 yr^{-1}.

Appendix B

In order to help interpret the discrepancy between peaks in the power spectra and recognizable frequencies, we carry out power spectrum analyses of many simulations of time series comprised of random noise plus a stable sinusoidal modulation.

We first examine modulations with frequency 1 yr^{-1}. We adopt the form

$$x_n = \text{randn} + D\sin(2\pi\nu_0 t_n), \qquad (B.1)$$

where randn denotes a normal random distribution with mean zero and standard deviation unity, $\nu_0 = 1$ and we consider a 10% depth of modulation, i.e., $D = 0.1$. We create 1,000 simulations and form the Lomb-Scargle power spectra. The mean and standard deviation of the resulting power spectra are shown in Figure 17. The peak is at 1 yr^{-1}, as expected, and we find that the half-height half-width is 0.03 yr^{-1}. This is close to the salient peak in the power spectrum of the time-distribution of trials, as shown in Figure 16. This corresponds to the Nyquist frequency appropriate to a uniform time series of duration 1/(2 X 0.03) yr, i.e., about 17 yr, which is comparable with the duration shown in Figure 15.

We have repeated this calculation for $\nu_0 = 24.74$, and the result is shown

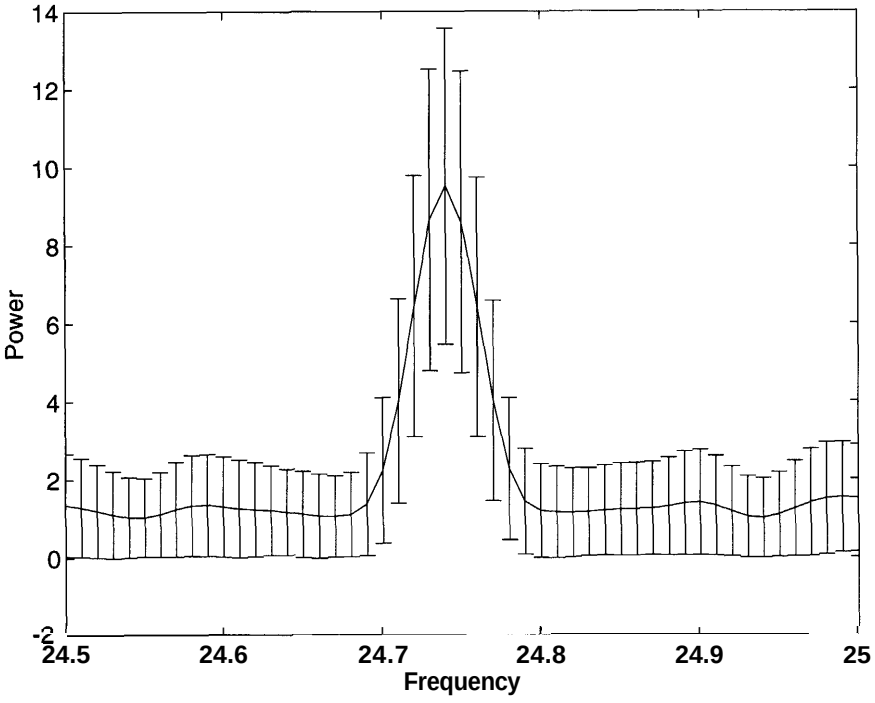

Fig. 18. Error-bar display of power spectra formed from 1,000 Monte Carlo simulations of time series with 10% depth of modulation at frequency 26.74 yr^{-1}.

in Figure 18. The shape of the power spectrum appears to be identical to that shown in Figure 17.

References

Allen, C. W. (1973). *Astrophysical Quantities* (p. 297). Athlone Press, London, UK. 1976.

Bretthorst, G. L. (1988). Bayesian spectrum analysis and parameter estimation. In Berger, J., Fienberg, S., Gani, J., Krickeberg, K., & Singer, B. (Eds.) *Lecture Notes in Statistics* (Vol. 48), Springer-Verlag.

Fraser-Smith, A. C. (1982). Is there an increase of geomagnetic activity preceding total lunar eclipses? *J. Geophys. Res., 87,* 895.

Lomb, N. (1976). Least-squares frequency analysis of unequally spaced data. *Astrophys. and Space Science, 39,* 447.

Mardia, K. V. (1972). *Statistics of Directional Data* (New York: Academic).

Radin, D. I., & Rebman, M. (1994). Lunar correlates of normal, abnormal, and anomalous human behavior. *Subtle Energies and Energy Medicine, 5,* 209.

Scargle, J. D. (1982). Studies in astronomical time series analysis. II. Statistical aspects of spectral analysis of unevenly spaced data. *Astrophys.* J., 263, 835.

Spottiswoode, S. J. P. (1997). Apparent association between effect size in free response anomalous cognition experiments and local sidereal time. *Journal of Scientific Exploration, 11,* 109.

Sturrock, P. A. (2004). Time-series analysis of a catalog of UFO events: evidence of a local-sidereal-time modulation. *Journal of Scientific Exploration, 18,* 399.